Iraqi Journal of Physics, 2021 *Vol.19, No.48, PP. 52-65*

DOI: 10.30723/ijp.19.48.52-65

Studying the Correlation between Supermassive Black Holes and Star Formation Rate for Samples of Seyfert Galaxies (Type 1 and 2)

Salwa Haithem Kareem, Y. E. Rashed

Department of Astronomy and Space, Collage of Science, University of Baghdad, Baghdad, Iraq

E-mail: salwahaithem@yahoo.com

Corresponding author: yassir.e@sc.uobaghdad.edu.iq

Abstract

A studying of the optical spectroscopic is reported in this work to investigate the correlation between the supermassive black hole (SMBH) and the star formation rate (SFR) for samples of Seyfert galaxies type (I and II). The study focused on 45 galaxies of Seyfert 1, in addition to 45 galaxies of Seyfert 2, where these samples were selected from different surveys of Salon Digital Sky Survey (SDSS). the range of red shift for these objects was between (0.02 – 0.26). The results of Seyfert 1 galaxies showed good correlation between the SMBH and the SFR depending on the statistical analysis parameter named Spearman's Rank Correlation in a factor of (ρ=0.609)In addition, the Seyfert 2 galaxies results showed good correlation between the SMBH and the SFR in a factor of (ρ=0.551). Moreover, the different types of line-regressions were fitted between the data (e.g. linear, exponential, and power) to choose the more suitable line among the data and to extract a mathematical formula that explains this behavior.

Key words

Galaxies – Techniques, spectroscopy, Active galaxies, Seyfert.

Article info.

Received: Oct. 2020
Accepted: Jan. 2021
Published: Mar. 2021

دراسة العلاقة بين الثقوب السوداء فائقة الكتلة و معدل تشكيل النجوم لنماذج من مجرات السيفرت (النوع الاول والثاني)

سلوى هيثم كريم، ياسر عز الدين رشيد

قسم الفلك والفضاء، كلية العلوم، جامعة بغداد، بغداد، العراق

الخلاصة

الدراسة الطيفية البصرية ذكرت في هذا البحث لدراسة العلاقة بين الثقوب السوداء فائقة الكتلة ومعدل تكوين النجوم لعينات من مجرة السيفرت النوع (الاول والثاني). ركزت الدراسة على 45 مجرة من السيفرت1 بالاضافة الى 45 مجرة من سيفرت2، حيث تم اختيار هذه العينات من مسح مختلف لـ Salon Digital Sky Survey (SDSS). ان الانزياح الاحمر لهذه الاجسام كان بين (0.26 – 0.02). النتائج لمجرة السيفرت1 اظهرت ان هناك علاقة جيدة بين الثقوب السوداء ومعدل تكوين النجوم اعتمادا على معامل تحليل احصائي يسمى (Spearman's Rank Correlation) في المعامل (ρ=0.609)، وكذلك نتائج مجرة سيفرت 2 اظهرت علاقة جيدة بين الثقوب السوداء ومعدل تكوين النجوم في معامل (ρ=0.551). علاوة على ذلك، تم تركيب أنواع مختلفة من انحدار الخط بين البيانات (مثل الخطي، الأسي، والقوة) لاختيار الخط الأكثر ملائمة بين البيانات واستخراج الصيغة الرياضية التي تشرح هذا السلوك.

Introduction

Seyfert galaxies are one of the main types of active galaxies I. It is divided into two subtypes: Seyfert type-I and Seyfert type-II. This division depends on the broadening of the emission-lines of their spectra. Where the widths of the forbidden and permitted emission-lines on the spectra of Seyfert 1 galaxies are up to ~ 10 000 km s^{-1}, while the emission-lines for Seyfert 2 galaxies have widths of < 1000 km s^{-1} [1]. Luminosity of seyfert galaxies varies over time. In the long time, 20% is the normal variation between the nuclear luminosity of most active galaxtic nuclei (AGN) and mean luminosity with an amplitude was described [2].

Imaging and spectroscopy are used to know the difference between the narrow line regions (NLRs) in Seyfert 1 and Seyfert 2 galaxies, Attendance or nonattendance of broad permitted lines with widths of 10^3 km s^{-1} or higher is the main different between two types of Seyfert galaxies [3].

The supermassive black hole (SMBH) is the major power source of the galaxies. This region exhibits high gravity that will not allow any particles or electromagnetic radiation to escape from it. The gas dynamic and stellar is the way to measure the MBH for near inactive galaxies, but in the case of active galaxies, further employing of reverberation mapping (RM) methods are needed to measure the mass of black hole [4].

Strongly star-forming (SFR) galaxies can be characterized spectroscopically by their emission line ratios. The source of SFR is the dense molecular clouds, therefore the gas content is an indication of the activity of star formation. The knowledge about the correlation between SMBH and SFR is not clear because is not yet fully understood. This is due to the fact that strong observational evidences that may help to understand the processes are still missing in many cases.

In this paper, the sections will be organized as follow: Section One and Two: presents the data collection and the data reduction of the samples that have been used in this work. Section Three: states the mathematical models that were used to calculate the central black holes for the Seyfert galaxies type1 and type2, as well as the mathematical calculations for the star formation rate (SFR). Section Four: will explain the statistical analysis that has been used in this paper to choose the best line regression. Section Five: will present the calculated results. Finally, in Section six: the discussion of the correlation between the supermassive black hole (SMBH) and the SFR for the samples used in this work is presented, in addition to the conclusions.

Data collection and data reduction

This section states the way to the data was collected depending on salon digital sky survey (SDSS). Additionally, the steps of data reduction (e.g. subtract the Fe II, fitting the power, fitting the emission-lines …etc) are explained.

1. Data collection

This project studied one type of the active galaxies named Seyfert galaxies. For each type of these galaxies 45 galaxies were collected, as listed in Table (1 and 2). These data were collected from different Salon Digital Sky Surveys (SDSS).

The SDSS will supply the data to support in detail investigations for the allocation of the luminous and nonluminous matter in the universe: a astrometrically and photometrically inspect digital imaging survey of π sr above about Galactic latitude 30° in five broad optical bands to a depth of ğ~23mag, and a spectroscopic scanning of the approximately 10^5 brightest quasars and 10^6 brightest galaxies found in the catalog of the photometric object that generated by the imaging survey. The SDSS will create both spectroscopic surveys and imaging over a large area of the sky [5]. SDSS is one of the best surveysfor studying the optical properties of active galactic nuclei (AGN), it has [6]:

• Exact and profound five-band photometry using a filter system prepared for optimal distinguish between quasars and stars.

• High S/N R(Signal-to-noise ratio) ~ 2000 spectra of close to 100,000 quasars with redshifts between zero and 5.5 coverage 3800−9200°A and with perfect spectrophotometric calibration

• Same quality spectra of a flux-limited sample of close to a million galaxies with redshifts below 0.2, give detailed emission-line studies of AGN.

2. Data reduction

The physical measurements cannot be extracted directly from the optical spectra of the galaxies due to the raw spectrum contain $Fe_{[ii]}$ emission line, power low, as well as stellar continue all these parameters should be subtracted. These spectra should go through several steps (e.g. extract the stellar continuum, the power, the Fe II line,etc) have to be performed. To do these corrections a Python pipeline has been used and modified by us to fit the sample that was used in this work. This pipeline was published by Guo et al. and Shen et al. [7, 8]. This code can calculate the information of the flux density of the emission lines, dispersion velocity (σ), and the full width at half max (FWHM). As mentioned, we had modified a Python pipeline to correct the Seyfert galaxies spectra depending on several stages as shown in Fig.1 and 2 [7, 8]. These corrections steps are summarized as follows:

First step: subtract the Fe_{II} emission-lines from spectrum.

Second step: subtract the stellar continuum.

Third step: a power-low template should be fitted on the spectra of Seyfert galaxies to settle down the original spectrum to zero-level then the flux density of the emission-lines requested in this research can be measured.

Fourth step: a narrow or broad Gaussian line is fitted depending on the broadening of the emission-lines to measure the flux density (f_v) and the FWHM of these fitted lines.

Two component Gaussian lines may need to be fitted depending on the complexity of these lines, e.g. the Hα permit-line as present in Fig.1 and 2.

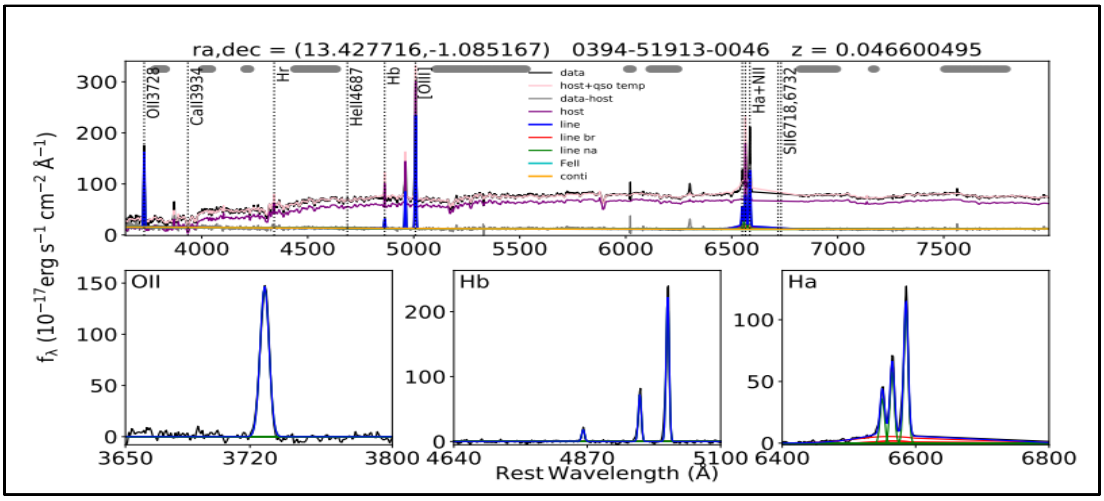

***Fig.1:** Spectral modeling for seyfert galaxies type1. The observed galaxy is shown in black line. The staller continuum is shown in faint brown line. The fitting component is in different colors. Fe_{II} present in teal color.*

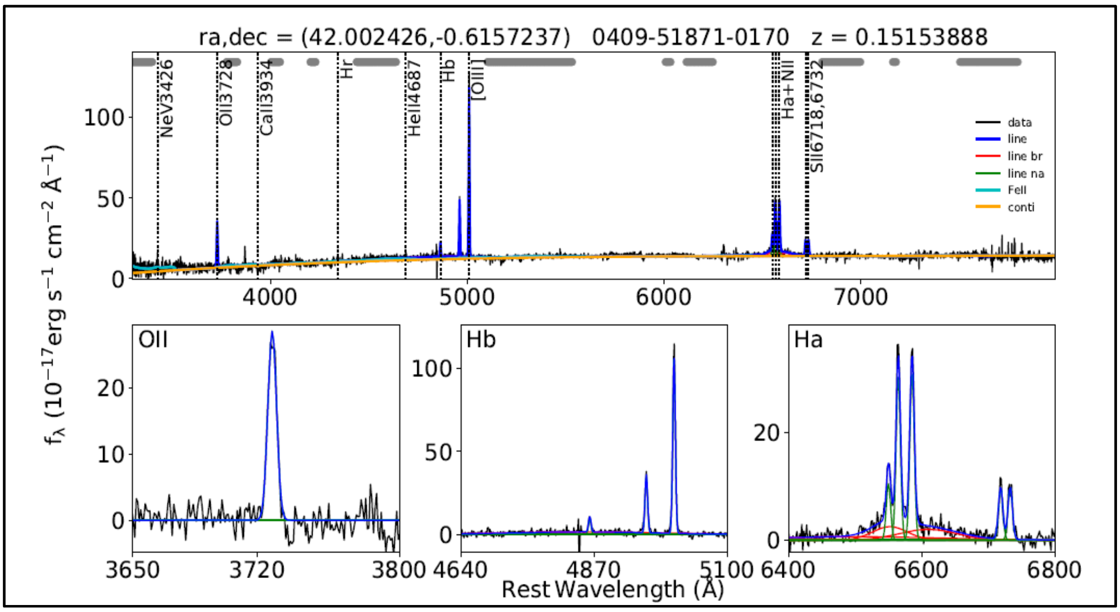

Fig.2: Spectral modeling for seyfert galaxies type2. The observed galaxy is shown in black line. The staller continuum in faint brown line. The fitting component are shown in different colors. Fe_{II} in teal color.

3. The Mathematical Model to Calculate the Central Black holes Masses and The Star Formation Rate

In this section, the mathematical equations that were used in this research, to calculate the SMBH and the SFR, are discussed.

3.1 Calculation the Super massive Black Hole

Many science articles refers that there are supermassive black holes lying at their center to hold all galaxies part together [1].

The following formula is used to estimate the central black hole mass via measuring the dispersion velocity (σ∗) of the gas cloud that surround the SMBH [9]:

$$\log \frac{M_{BH}}{M_\odot} = 8.12 + \log\left(\frac{\sigma *}{200\ km.S^{-1}}\right)^{4.24\pm0.41} \qquad (1)$$

The following formula is used to calculate the dispersion velocity (σ_*) from FWHM of $[O_{III}]$ [10]:

$$\sigma_* = \frac{(\sqrt{FWHM[O_{III}]})^2 - (150)^2/2.35}{1.34} \qquad (2)$$

3.2 Star formation rate calculation

Star formation is one of the most important phenomena during the formation of a galaxy. To measure the star formation rate (SFR), the luminosities of $[O_{II}]$ were used because they depend on the ionizing photon luminosity [11].

$$\mathrm{SFR}_{[O\ II]}\ [M_\odot\ yr^{-1}] = \frac{L_{[O_{II}]}}{2.97 \times 10^{33} W} \qquad (3)$$

To calculate the luminosities of $[O_{II}]$ [12]:

$$L_{[O_{II}]} = 4\pi \times D_L \times S \qquad (4)$$

where D_L is luminosity distance in units(MPc) and S is the flux density for each $[O_{II}]$ line in units(erg. cm^{-2}. s^{-1}**)** The luminosity distance D_L has been calculate for each galaxy by combining the redshift with the cosmology constants H_0 = 70 km s^{-1} Mpc^{-1}, Ω_m = 0.3($Omega_{M}$), and Ω_Λ = 0.7($Omega_{vac}$) [13].

4. Statistical analysis of the data

In order to reach accurate results regarding the extent correlation between the calculated physical properties, as well as choosing the best line regression, the following statistical analysis methods were applied.

a. Spearman's rank correlation

Spearman's rank correlation test is used in astronomy to find if there a correlation between two variable or not. The Spearman's rank correlation coefficient does not try to evaluate the errors on its value. The Spearman's rank correlation coefficient ρ for the sample is calculated from the square of the difference of the two ranks for each pair by [14]:

$$\rho = 1 - \frac{6\sum_{i=1}^{N}(RXi - RYi)2}{N(N^2-1)} \qquad \textbf{(5)}$$

where ρ The Spearman's rank correlation coefficient, *N* is the number of data pairs, *RXi* and *RYi* is an ascending order rank.

4.2 Coefficient of Regression (R-Squared)

R-Squared is a statistical measurement for the data points of the experiment, and how close these data are to the regression fitted line. Moreover, it also recognizes the Coefficient of Regression. The value of R^2 is between the (0 – 1). The best value is close to 1, which means that the fitting model explain the variability of the responding points nearly its mean. Calculation of R^2 is done by applying the following formula [15]:

$$\boldsymbol{R^2 = 1 - \frac{SS_{RES}}{SS_{TOT}} = 1 - \frac{\sum_i\left(Y_i - \widehat{Y}_i\right)^2}{\sum_i(Y_i - \overline{Y}_i)^2}} \qquad (6)$$

where SS_{RES} represents the summation of the vertical distance points from the best regression, and SS_{TOT} represents the summation of the squares points of the vertical range from the horizontal bar dragged at the mean Y value.

Results and discussions

The data in this work had been divided into two groups. The first one, represents all the samples, (45) galaxies, for each type of Seyfert. The second group represents the median values. Spearman's rank correlation was applied a on each group of the data. It was found that the value of this coefficient for all the data of seyfert1 galaxies was (0.609) and for median values of seyfert1 galaxies is (0.929). While for seyfert2 galaxies, the value of Spearman's rank correlation was (0.551) for all data, and for median values of seyfert2 galaxies was (0.929). These values give an indication to the strong correlation between SMBH and SFR for both types.

The data of Seyfert type-I galaxies with the redshift 0.259≥ z ≥ 0.041 are listed in Table 1 that contains 45 objects. While the redshift of (45) Seyfert type-II galaxies was between (0.02 – 0.26), and it is listed in Table 2.

Table 1: The data for Sy1 galaxies.

No	Name of the Sources	Coordinate		Redshift (z)	D_L	σ [O_{III}] (km/s)	Flux density of [O_{II}] [10^{-17}erg. cm^{-2} . s^{-1}]	$log\frac{M_{BH}}{Mo}$	SFR$_{[OII]}$ [M⊙ yr^{-1}]
		RA	DE						
1[16]	2SLAQ J0001.27+0007.4	00 01 54.276	00 07 32.457	0.139	656.3	106.796	292.801	5.4	5.079
2[16]	2MASX J0002-1030	00 02 02.961	-10 30 38.063	0.102	470.1	186.943	229.849	7.8	2.045
3[16]	2MASS J0007+1554	00 07 03.611	15 54 23.675	0.114	529.6	185.190	665.712	7.7	7.519
4[16]	2MASX J0042+1509	00 42 41.907	15 09 26.193	0.101	465.2	137.251	95.171	6.5	0.829
5[16]	SDSS J0010.25-0901.0	00 10 56.255	-09 01 09.973	0.081	368.1	145.808	117.622	6.7	0.641
6[16]	2MASX J0018+0107	00 18 52.472	01 07 58.449	0.063	282.7	104.630	111.680	5.3	0.359
7[16]	2MASX J00405+1533	00 40 55.887	15 33 49.078	0.099	455.4	141.481	136.198	6.6	1.137
8[16]	2MASX J0042-1049	00 42 36.863	-10 49 22.096	0.041	181.1	134.550	1407.737	6.4	1.859
9[16]	SDSS J0036.78+0105.3	00 36 59.782	01 05 44.332	0.121	564.7	121.299	125.734	5.9	1.614
10[16]	SDSS J0059.19+1436.2	00 59 50.190	14 36 48.223	0.187	909.4	118.218	89.737	5.8	2.988
11[16]	2MASX J0053-0105	00 53 42.642	-01 05 06.619	0.046	203.9	161.709	889.927	7.2	1.490
12[16]	CAIRNS J0053.10-0010.8	00 53 03.098	-00 10 46.717	0.138	651.2	102.5178	74.427	5.2	1.271
13[16]	SDSS J0045.72+1442.9	00 45 24.722	14 42 45.902	0.195	952.8	220.156	155.230	8.5	5.675
14[16]	NGC 617	01 34 02.537	-09 46 26.949	0.040	176.5	137.224	392.465	6.5	0.492
15[16]	GAMA 218688	09 18 25.794	00 50 58.442	0.086	392.1	129.897	226.610	6.2	1.403
16[16]	2MASX J0918+3554	09 18 23.000	35 54 38.747	0.084	382.5	180.474	160.440	7.6	0.945
17[16]	SDSS J0917.89+0718.0	09 17 53.893	07 18 34.030	0.091	416.3	133.064	104.979	6.3	0.732
18[16]	GAMA 388235	09 16 55.207	02 30 43.406	0.139	656.3	156.853	84.876	7.0	1.472
19[16]	SDSS J0917.88+3704.1	09 17 12.888	37 04 32.133	0.159	760.2	117.586	100.037	5.8	2.328
20[16]	2MASX J0917+27197	09 17 28.570	27 19 50.977	0.070	315.7	161.065	363.033	7.2	1.457
21[16]	2MASS J0919+6344	09 19 03.410	63 44 49.725	0.116	539.6	110.878	158.102	5.6	1.853
22[16]	2MASX J0919+55272	09 19 13.201	55 27 55.004	0.048	213.1	189.014	3399.967	7.8	6.218
23[16]	3C 219	09 21 08.626	45 38 57.345	0.174	839.6	316.627	456.804	10.0	12.968
24[16]	2MASS J0921+1652	09 21 32.632	16 52 57.022	0.095	435.8	175.384	1054.616	7.5	8.066
25[16]	SDSS J0154.37-0947.4	01 54 12.377	-09 47 32.565	0.193	941.9	123.080	33.406	6.0	1.193
26[16]	SDSS J0052.57+0035.2	00 52 00.563	00 35 49.307	0.114	529.6	132.349	85.321	6.3	0.963
27[17]	UGC 793	01 14 48.677	-00 29 46.098	0.033	144.9	128.378	407.185	6.2	0.344
28[18]	SDSS J0034.26-0859.6	00 34 18.270	-08 59 00.675	0.157	749.7	162.148	167.440	7.2	3.790
29[18]	2MASS J0032-0100	00 32 38.199	-01 00 35.330	0.091	416.3	96.947	185.290	5.0	1.293
30[18]	2MASS J0028+1452	00 28 48.771	14 52 16.248	0.089	406.6	123.050	196.050	6.0	1.300
31[18]	2MASS J0001-1023	00 01 02.185	-10 23 26.905	0.292	1505.1	165.745	184.104	7.3	16.796
32[18]	2MASX J0003+1602	00 03 38.943	16 02 20.672	0.116	539.6	164.257	301.094	7.2	3.530
33[18]	2MASX J0011+1442	00 11 37.246	14 42 01.400	0.132	620.5	241.179	328.901	8.9	5.1000
34[18]	2SLAQ J0008.22-0057.3	00 08 13.225	-00 57 53.312	0.139	656.3	625.923	721.447	12.9	12.515
35[19]	[VV2003c] J0002.5-1103	00 02 18.560	-11 03 57.265	0.205	1007.5	157.126	69.021	7.0	2.821
36[19]	[VV2003c] J0000.2-0954	00 00 48.161	-09 54 04.136	0.205	1007.5	150.115	128.333	6.9	5.246
37[19]	2MASS J0002+0045	00 02 49.070	00 45 04.858	0.086	392.1	375.328	451.607	10.7	2.796
38[20]	2MASS J0051+1354	00 51 18.282	13 54 48.114	0.137	646.0	114.176	126.163	5.7	2.120
39[20]	2MASS J0029+1508	00 29 59.037	15 08 17.218	0.210	1035.0	208.007	91.882	8.2	3.964
40[20]	2MASS J0033-1019	00 33 19.524	-10 19 24.023	0.259	1311.9	221.983	126.786	8.5	8.788
41[20]	2MASX J0049+1532	00 49 30.895	15 32 16.377	0.240	1203.1	184.501	274.502	7.7	16.001
42[20]	2MASX J0306+00034	03 06 39.575	+00 03 43.150	0.107	494.8	264.735	477.352	9.3	4.706
43[21]	2MASXJ0948+4030	09 48 38.426	40 30 43.815	0.047	208.5	133.462	249.554	6.4	0.436
44[21]	6dFGS gJ0310.9-0049	03 10 27.826	−00 49 50.803	0.080	363.3	98.735	244.895	5.1	1.301
45[21]	2MASXJ1543+3631	15 43 51.450	+36 31 36.755	0.067	301.5	186.785	762.368	7.8	2.791

Table 2: The data for Sy2 galaxies.

No	Name of the Sources	Coordinate		Redshift (z)	D_L	σ [O_{III}] (km/s)	Flux density of [O_{II}] [10^{-17}erg. cm^{-2}. s^{-1}]	$log\frac{M_{BH}}{Mo}$	$SFR_{[OII]}$ [$M_\odot$ yr^{-1}]
		RA	DE						
1[16]	IC 5287	23 09 20.268	00 45 23.408	0.032	140.4	93.929	245.009	4.9	0.194
2[16]	2MASX J2253+0048	22 53 31.410	00 48 25.474	0.072	325.1	188.109	431.607	7.8	1.837
3[16]	2MASX J2253-0825	22 53 06.458	-08 25 19.392	0.059	264.0	157.888	370.229	7.1	1.039
4[16]	2MASX J2228-0053	22 28 57.7126	-00 53 50.839	0.058	259.3	122.307	229.817	6.0	0.622
5[16]	2MASX J1729+5429	17 29 35.816	54 29 40.057	0.081	368.1	147.523	124.459	6.8	0.679
6[16]	2MASX J1722+3006	17 22 23.358	30 06 25.826	0.091	416.3	129.162	439.129	6.2	3.064
7[16]	2MASX J1707+3056	17 07 43.364	30 56 18.172	0.082	372.9	125.951	146.933	6.1	0.822
8[16]	2MASX J1641+2249	16 41 07.640	22 49 24.776	0.034	372.9	125.796	802.493	6.1	0.721
9[16]	MCG+04-39-016	16 34 53.667	23 12 42.664	0.038	149.4	152.104	925.309	6.9	1.045
10[16]	2MASX J1633+1154	16 33 35.303	11 54 23.914	0.103	167.5	141.686	302.802	6.6	2.752
11[16]	2MASX J1633+4157	16 33 06.838	41 57 40.283	0.137	475.1	304.655	259.192	9.9	4.356
12[16]	2MASX J0039-0032	00 39 16.414	-00 32 32.814	0.109	504.7	143.112	222.506	6.7	2.282
13[16]	2MASX J0121+1500	01 21 08.191	15 00 11.429	0.054	240.8	130.221	221.242	6.3	0.516
14[16]	MCG-02-05-022	01 37 06.955	-09 08 57.362	0.069	310.9	280.282	531.817	9.5	2.071
15[16]	2MASX J0210-0903	02 10 11.493	-09 03 35.447	0.041	181.1	188.655	2031.487	7.8	2.683
16[16]	2MASX J0248-0036	02 48 00.586	-00 36 56.650	0.151	718.4	138.598	163.978	6.5	3.408
17[16]	Mrk 609	03 25 25.359	-06 08 37.938	0.034	149.4	251.779	3129.974	9.0	2.813
18[16]	2MASS J0749+3039	07 49 42.054	30 39 51.370	0.156	744.5	124.622	197.677	6.1	4.412
19[16]	MASX J0756+4451	07 56 43.726	44 51 24.183	0.049	217.7	135.113	306.443	6.4	0.584
20[16]	2MASX J0757+3459	07 57 51.196	34 59 21.776	0.070	315.7	158.526	296.766	7.1	1.191
21[16]	2MASX J0801+4516	08 01 17.562	45 16 52.908	0.130	610.3	189.847	533.038	7.8	7.995
22[16]	2MASX J0804+4048	08 04 03.408	40 48 09.297	0.126	590.0	146.223	224.861	6.7	3.152
23[16]	SDSS J0805.29+2818.7	08 05 23.300	28 18 15.700	0.128	600.1	353.869	694.369	10.5	10.071
24[16]	2MASX J0848+1417	08 48 46.987	14 17 29.768	0.093	426.1	141.337	151.531	6.6	1.108
25[16]	2MASX J0859+3847	08 59 31.855	38 47 54.120	0.093	426.1	165.980	258.743	7.3	1.891
26[16]	2MASX J0908+2717	09 08 08.317	27 17 53.513	0.082	372.9	119.945	238.261	5.9	1.334
27[16]	LEDA 1044612	03 54 30.321	-05 26 53.089	0.109	504.7	144.992	182.985	6.7	1.877
28[17]	2MFGC 475	00 39 48.411	-09 08 34.00	0.037	162.9	116.345	272.426	5.8	0.291
29[17]	2MFGC 913	01 13 33.063	00 29 48.189	0.044	194.8	132.539	94.058	6.3	0.143
30[17]	Mrk 955	00 37 35.797	00 16 50.470	0.034	149.4	138.489	810.300	6.5	0.728
31[17]	NGC 856	02 13 38.358	-00 43 02.284	0.020	87.0	146.193	1111.934	6.7	0.338
32[17]	NGC 905	02 22 43.558	-08 43 08.100	0.045	199.3	146.931	209.002	6.8	0.334
33[18]	MCG+08-15-009	07 51 51.880	49 48 51.490	0.024	104.7	151.708	1595.274	6.9	0.704
34[18]	2MASX J0859+1001	08 59 22.636	10 01 32.239	0.166	797.1	214.154	136.528	8.4	3.493
35[18]	2MASX J0923+2946	09 23 19.728	29 46 09.078	0.062	278.0	99. 456	253.595	5.1	1.181
36[18]	2MASX J0936+2733	09 36 28.670	27 33 20.856	0.103	475.1	132.232	167.803	6.3	1.525
37[18]	2MASX J1125+4353	11 25 32.963	43 53 54.166	0.121	564.7	121.873	73.418	6.0	0.942
38[18]	2XMM J1000.1+5536	10 00 32.242	55 36 30.941	0.215	1062.7	164.463	231.124	7.2	10.51
39[18]	2MASX J1005+0547	10 05 38.288	05 47 26.815	0.123	574.8	203.658	300.313	8.1	3.996
40[18]	SDSS J1020. 81+6424.8	10 20 39.823	64 24 35.888	0.122	569.8	143.241	467.447	6.7	6.112
41[18]	SDSS J0003.82-0101.9	00 03 51.828	-01 01 41.990	0.268	1364.1	235.645	176.510	8.8	13.22
42[19]	2MASX J0000+0035	00 00 26.311	00 35 50.878	0.103	475.1	211.158	236.607	8.3	2.151
43[19]	2MASX J0001-0014	00 01 30.242	-00 14 46.447	0.088	401.8	137.784	171.334	6.5	1.114
44[19]	2MASX J0806+2004	08 06 41.662	20 04 58.424	0.145	687.2	141.497	83.294	6.6	1.584
45[19]	2MASX J0810+3451	08 10 13.012	34 51 36.840	0.082	372.9	145.536	246.793	6.7	1.382

Three different types of regression (Linear, Exponential, and Power-Low) were applied through the data in this research. The best fitting parameters as well as the statistical analysis values for Sy1 and Sy2 galaxies are presented in Table 3 and 4.
The main idea of this work is to find if there is a correlation between the SMBH and SFR for the main types of Seyfert galaxies (I and II), and how is the goodness of these correlations. Three types of regressions were fitted via the calculated parameters of SMBH vs SFR as follows:

1. Linear regression

Fig.3 (a) represents the correlation between the SMBH and SFR using linear model for seyfert1 galaxies, where the goodness of the correlation was R^2= 0.31. To be more accurate about the linear regression, a median calculation was applied through the data as shown in Fig.3 (b), and the goodness of the correlation was R^2= 0.94. All the above indicates strong correlation between the variables.
The linear formula for Sy1 is:

$$\boldsymbol{f_{(x)} = a \times x + b} \quad \textbf{(7)}$$

All samples ➔ $\boldsymbol{SFR = (1.26 \pm 0.36)SMBH + (-7.70 \pm 2.61)} \quad \textbf{(8)}$

Median ➔ $\boldsymbol{SFR = (1.52 \pm 0.17)SMBH + (-8.01 \pm 1.57)} \quad \textbf{(9)}$

The correlation between SMBH and SFR for seyfert2 galaxy using linear models is shown in Figs.4 (a and b). Where the goodness of correlation (R^2) for all samples and the median were (0.305 and 0.711), respectively.
The linear formula for Sy2 is:

All samples ➔ $\boldsymbol{SFR = (1.44 \pm 0.31)SMBH + (-7.59 \pm 2.27)} \quad \textbf{(10)}$

Median ➔ $\boldsymbol{SFR = (1.42 \pm 0.40)SMBH + (-7.78 \pm 3.16)} \quad \textbf{(11)}$

Table 3: Best fitting parameters for Syfert1 galaxies.

Type	Spearman's Value	P	Type of fitting	a	b	R^2
Seyfert_1 normal	0.609	0.000	linear	1.62± 0.36	-7.79± 2.61	0.31
			exp	$2.06*10^{-04}$± $1.23*10^{-04}$	2.911± 0.626	0.12
			power	0.034±0.04	2.36±0.55	0.29
Seyfert_1 median	0.929	0.003	linear	1.52±0.17	-8.01±1.57	0.94
			exp	$6.87*10^{-05}$± $4.98*10^{-05}$	3.23± 1.025	0.71
			power	0.017± 0.012	2.57± 0.30	0.96

Table 4: Best fitting parameters for Syfert2 galaxies.

Type	Spearman's Value	P	Type of fitting	a	B	R^2
Seyfert_2 normal	0.551	0.000	linear	1.44±0.31	-7.59±2.27	0.305
			exp	$2.95*10^{-04}$±$1.11*10^{-04}$	1.77±$4.37*10^{-01}$	0.23
			power	0.004±0.006	3.25±0.69	0.302
Seyfert_2 median	0.929	0.003	linear	1.42±0.40	-7.78±3.16	0.711
			exp	$2.24*10^{-04}$±$5.26*10^{-05}$	1.11±$4.96*10^{-01}$	0.906
			power	$4.33*10^{-05}$±$1.45*10^{-04}$	5.19±1.45	0.85

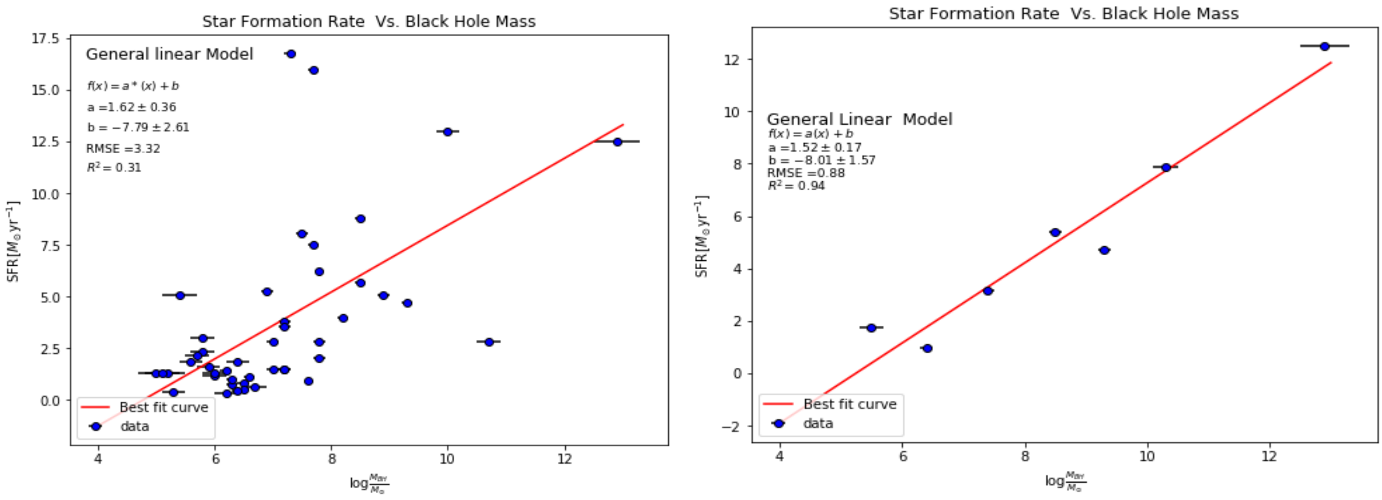

(a) **(b)**

Fig.3: The correlation between the SMBH & SFR for seyfert 1 galaxies using linear regression, where (a) for all samples, (b) median data.

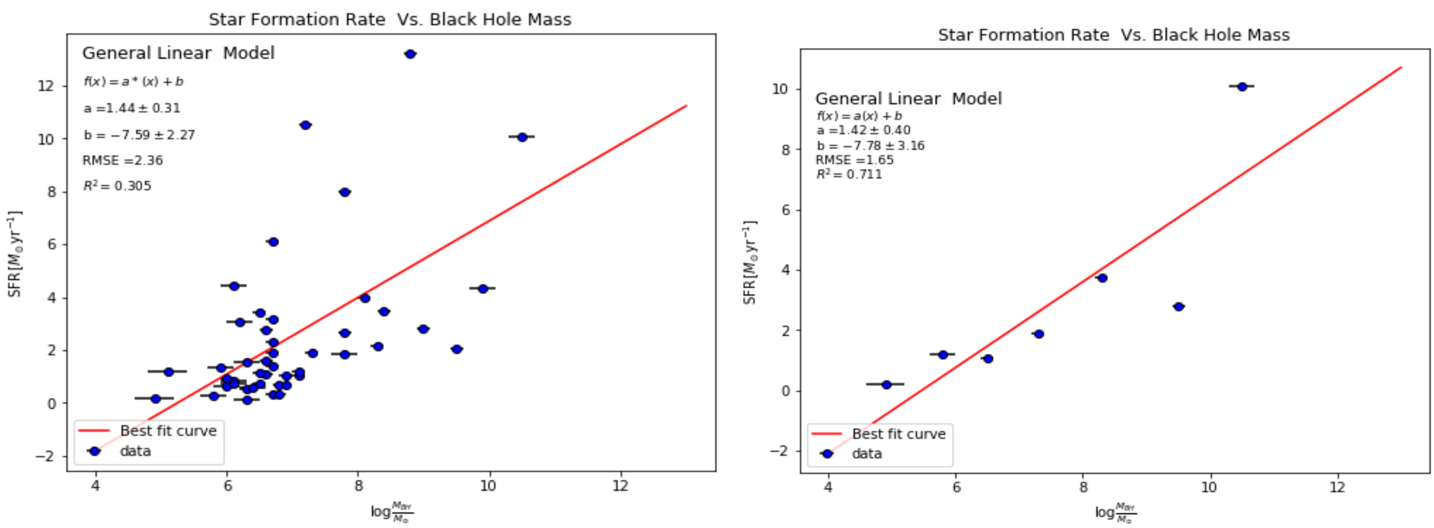

(a) **(b)**

Fig.4: The correlation between the SMBH & SFR for seyfert2 galaxies using linear regression, where (a) for all samples, (b) median data.

2. Exponential regression

In Figs.5 (a and b), an exponential regression was fitted for the correlation between SMBH vs SFR for Sy1 galaxies. The values of the fitting parameters are listed in Table 3. The goodness of this mathematical model was (0.12 and 0.71) for all data and median, respectively. The goodness of this mathematical model is lower than the linear model.

The exponential formula is:

$$\boldsymbol{f_{(x)} = a \times \exp(x) + b}$$

$$\textbf{All samples} \Rightarrow \boldsymbol{SFR = (2.06 \times 10^{-4} \pm 1.23 \times 10^{-4}) \times \exp(SMBH) + (2.911 \pm 0.626)} \quad (12)$$

$$\textbf{Median} \Rightarrow \boldsymbol{SFR = \left(6.87 \times 10^{-5} \pm 4.98 \times 10^{-5}\right) \times \exp(SMBH) + (3.23 \pm 1.025)} \quad (13)$$

Figs.6 (a and b) represent the correlation between the SMBH Vs SFR for syfert2 galaxies. The fitting parameters (a and b) were listed in Table 4. The goodness of the fitting (R^2) was (0.23) for all data, and (0.906) for median values. Here the exponential fitting explains well the variation between the data especially in Fig.6 (b). The exponential formula for Sy2 is:

$$\textbf{All samples} \Rightarrow SFR = (2.95 \times 10^{-4} \pm 1.11 \times 10^{-4}) \times \exp(SMBH) + (1.77 \pm 0.43) \quad (14)$$

$$\textbf{Median} \Rightarrow SFR = \left(2.24 \times 10^{-5} \pm 5.26 \times 10^{-5}\right) \times \exp(SMBH) + (1.11 \pm 0.49) \quad (15)$$

Note: The exponential model is the best fitting model to explain the correlation between SMBH and SFR for seyfert2 galaxies.

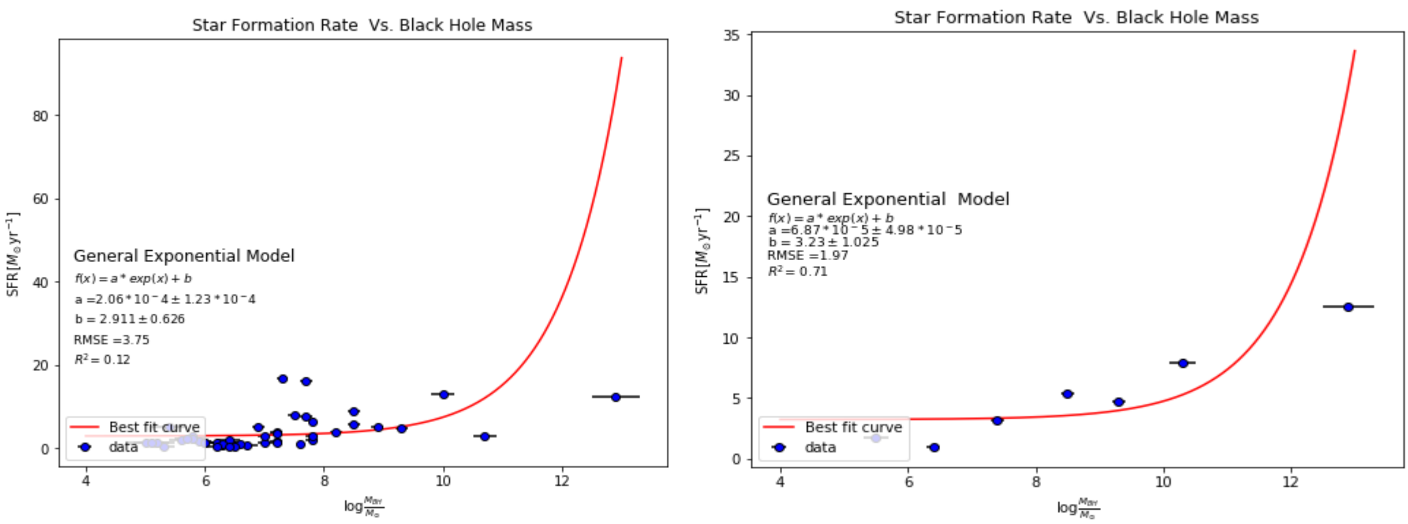

Fig. 5: The correlation between the SMBH & SFR for seyfert1 galaxies using exponential regression, where (a) for all samples, (b) median data.

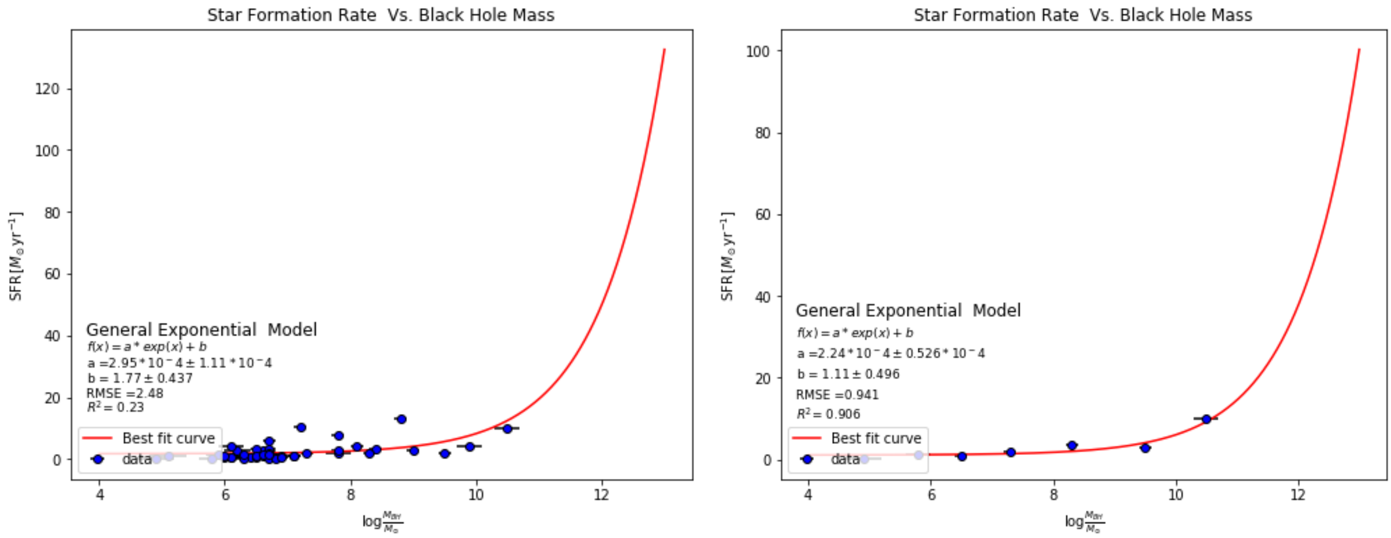

(a) (b)

Fig.6: The correlation between the SMBH & SFR for seyfert2 galaxies using exponential regression, where (a) for all samples, (b) median data.

Power-Low regression

Fig.7 (a and b) represent the power low fitting through the correlation between SMBH and SFR for seyfert1 galaxies. The fitting parameters are listed in Table 3. The goodness of this fitting is the best among the three mathematical models, especially on the median value, where the value of goodness (R^2) was (0.29) for all points, and for median it was (0.96). The previous results give an indication that the correlations between SMBH and SFR for sy1 galaxies are power low.

The formula of power low is:

$$\boldsymbol{f_{(x)} = a \times (x)^{b}}$$

All samples ➔ $\boldsymbol{SFR = (0.034 \pm 0.04) \times (SMBH)^{2.36 \pm 0.55}}$ **(16)**

Median ➔ $\boldsymbol{SFR = (0.017 \pm 0.012) \times (SMBH)^{2.57 \pm 0.30}}$ **(17)**

The correlation between SMBH vs SFR for Sy2 galaxies fitted by power low is shown in Figs.8 (a and b). Where the goodness of correlation is (0.302) for all data, while for median is (0.85). The fitting parameters of this mathematical model are presented in Table 4.

The power low formula for Sy2 galaxies is:

All samples ➔ $\boldsymbol{SFR = (0.004 \pm 0.006) \times (SMBH)^{3.25 \pm 0.69}}$ **(18)**

Median ➔ $\boldsymbol{SFR = (4.33 \times 10^{-5} \pm 1.45 \times 10^{-4}) \times (SMBH)^{5.19 \pm 1.45}}$ **(19)**

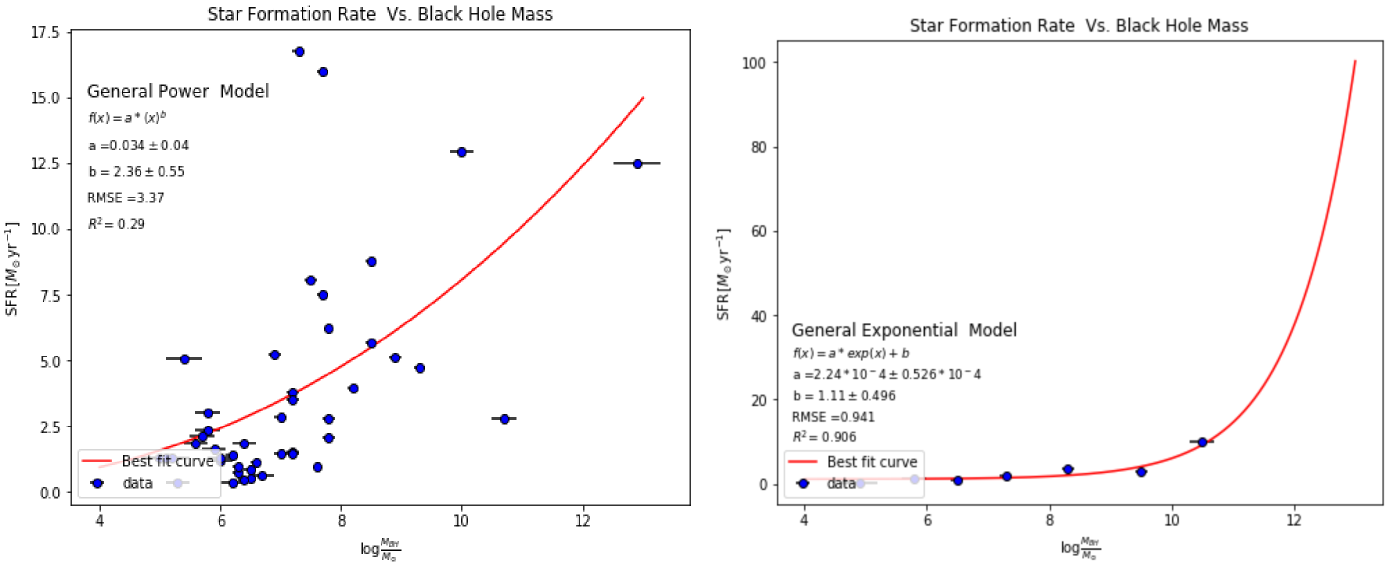

Fig. 6: The correlation between the SMBH & SFR for seyfert2 galaxies using exponential regression, where (a) for all samples, (b) median data.

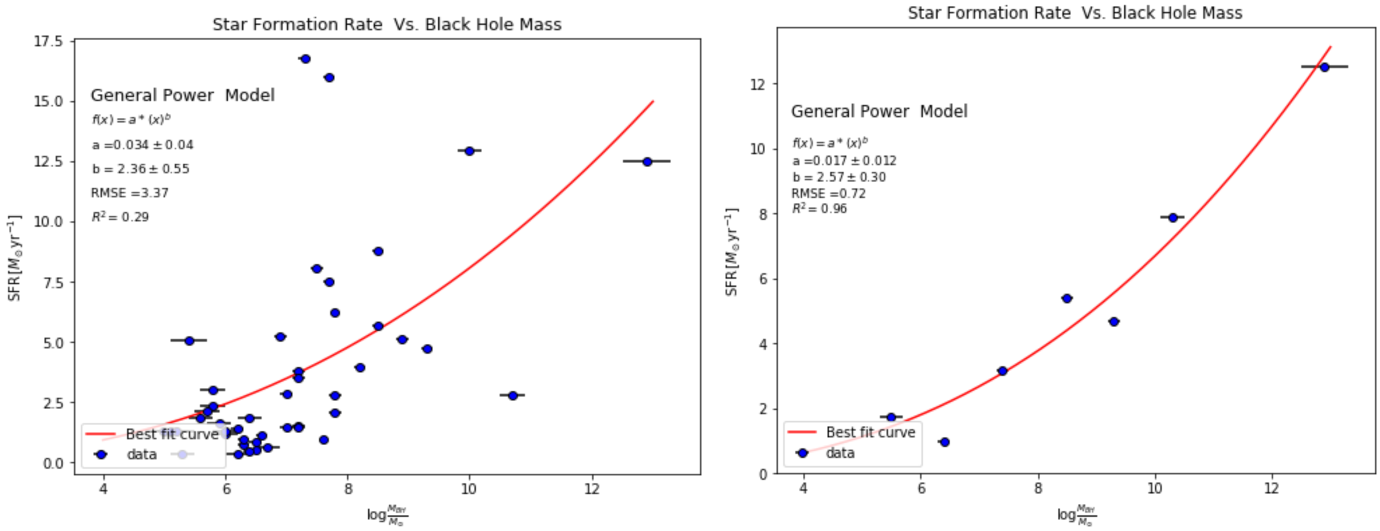

(a) **(b)**

Fig.7: The correlation between the SMBH & SFR for seyfert1 galaxies using power regression, where (a) for all samples, (b) median data.

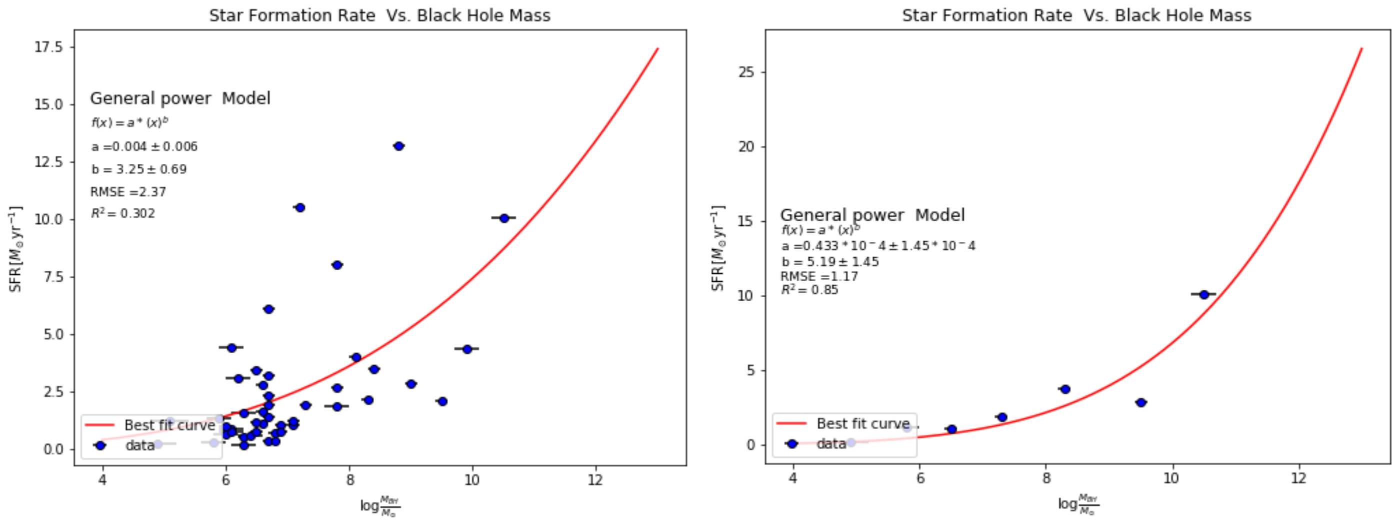

(a) **(b)**

Fig.8: The correlation between the SMBH & SFR for seyfert2 galaxies using power regression, where (a) for all samples, (b) median data.

Conclusions

The broad emission-lines in Seyfert1 galaxies are generated in the broad line region (BLR), where this area approximately located at 10^{11} km from the center of galaxy and the speed of the cloud in this region is 5000 km.S^{-1} [22]. While the radius of the narrow line region (the causes of narrow emission-lines) in Seyfert 2 galaxies are approximately from few Kpc to hundreds of Kpc [23]. Both these regions are highly affected by the central black holes. Therefore, it was noticed that the correlation between SMBH and SFR was higher in Sy1 than Sy2, as was clarified in section five.

According to the results presented in section five, as well as the statistical investigation of the three mathematical fitting models (Linear, Exponential, and Power-low),the followings can be conclude

1. There were good correlations between the SMBH and SFR for Seyferts in a factor of:
Sy1 ➔ ρ = 0.6
Sy2 ➔ ρ= 0.55

2. The best mathematical formula that controls the correlation between SMBH and SFR was:
a. Power-low for Sy1 galaxies as clarified in Eqs. (16 and 17).
b. Exponential for Sy2 galaxies as shown in Eqs. (14 and 15).

3. According to the histogram (Fig.9) that represents the distribution of SMBH of Seyferts, it was found that the masses of SMBH of Sy1 are larger than that of Sy2 in general. Furthermore, these results of the SMBH distribution matches those of the following references:
a. The black hole masses of Sy1 and Sy2 between 10^4 and 10^8 $M_\odot$ [24].
b. The black hole mass for Sy1 and Sy2 between 10^4 and 10^6 $M_\odot$ [25].
c. The black hole mass for Sy1 between 10^6 and 10^8 $M_\odot$ [26].

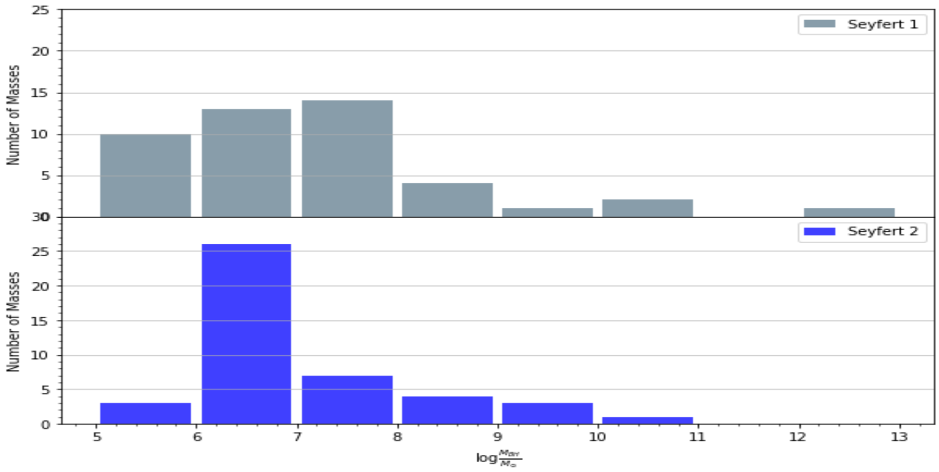

Fig.9: A histogram of SMBHs distributions for seyfert galaxies.

Acknowledgement

The authors would like to thank the SDSS team for free offer of their data.

References

[1] Y. E. Rashed, "The relation between variable active galactic nuclei, their immediate environments, and the conditions for star formation", Ph.D. Thesis, Doctoral dissertation, Universitäts-und Stadtbibliothek Köln (2015).

[2] H. Winkler, "Some things change, some don't. An exploration of Seyfert galaxy luminosity changes over a generation", heas, 11 (2017).

[3] M. A. Malkan, L. D. Jensen, D. R. Rodriguez, L. Spinoglio, B. Rush, The Astrophysical Journal, 846, 2 (2017) 1-26.

[4] C. J. Grier, A. Pancoast, A. J. Barth, M. M. Fausnaugh, B. J. Brewer, T. Treu, B. M. Peterson, The Astrophysical Journal, 849, 2 (2017) 1-18.

[5] F. D. Albareti, C. A. Prieto, A. Almeida, F. Anders, S. Anderson, B. H. Andrews, V. Avila-Reese, The Astrophysical Journal Supplement Series, 233, 2 (2017) 1-25.

[6] M. A. Strauss, Y. Shen, N. A Bahcall, P. B. Hall, In Panoramic Views of Galaxy Formation and Evolution, 399 (2008) 1-12.

[7] H. Guo, X. Liu, Y. Shen, A. Loeb, T. Monroe, J. X. Prochaska, Monthly Notices of the Royal Astronomical Society, 482, 3 (2019) 3288-3307.
[8] Y. Shen, P. B. Hall, K. Horne, G. Zhu, I. McGreer, T. Simm, C. J. Grier, The Astrophysical Journal Supplement Series, 241, 2 (2019) 1-16.
[9] J. H. Woo, C. M. Urry, The Astrophysical Journal, 579, 2 (2002) 530-544.
[10] J. E. Greene, L. C. Ho, The Astrophysical Journal, 627, 2 (2005) 721-732.
[11] C. W. Yip, A. S. Szalay, arXiv preprint arXiv:1110.0726, (2011) 1-14.
[12] K. M. Blundell, New Astronomy Reviews, 47, (6-7) (2003) 593-597.
[13] Roberto Serafinelli, Paola Severgnini, Valentina Braito, Roberto Della Ceca, Cristian Vignali, Filippo Ambrosino, Claudia Cicone, Alessandra Zaino, Massimo Dotti, Alberto Sesana, Vittoria E. Gianolli, Lucia Ballo, Valentina La Parola, and Gabriele A. Matzeu. The Astrophysical Journal, 902, 1 (2020) 1-11.
[14] P.A. Curran, arXiv preprint arXiv:1411.3816, (2014) 1-5.
[15] T. O. Kvålseth, The American Statistician, 39, 4 (1985) 279-285.
[16] K. Oh, K. Y. Sukyoung, K. Schawinski, M. Koss, B. Trakhtenbrot, K. Soto, The Astrophysical Journal Supplement Series, 219, 1 (2015) 1-17.
[17] E. Tempel, R. Kipper, A. Tamm, M. Gramann, M. Einasto, T. Sepp, T. Tuvikene, Astronomy & Astrophysics, 588, A14 (2016) 1-11.
[18] S. F. Anderson, B. Margon, W. Voges, R. M. Plotkin, D. Syphers, D. Haggard, P. B. Hall, The Astronomical Journal, 133, 1 (2007) 313-329.
[19] M. P. Véron-Cetty, P. Véron, Astronomy & Astrophysics, 518, A10 (2010) 1-8.
[20] R. Coziol, H. Andernach, J. P. Torres-Papaqui, R. A. Ortega-Minakata, Moreno del Rio, F. Monthly Notices of the Royal Astronomical Society, 466, 1 (2017) 921-944.
[21] J. N. Runco, M. Cosens, V. N. Bennert, B. Scott, S. Komossa, M. A. Malkan, D. Park, The Astrophysical Journal, 821, 1 (2016) 23-33.
[22] M. H. Jones and R. J. A. Lambourne, "An Introduction to Galaxies and Cosmology", Co-published with The Open University, Milton Keynes. Cambridge, UK: Cambridge University Press, (2004).
[23] N. Bennert, H. Falcke, H. Schulz, A. S. Wilson, B. J. Wills, The Astrophysical Journal, 574 (2002) L105-L109.
[24] F. Panessa, L. Bassani, M. Cappi, M. Dadina, X. Barcons, F. J. Carrera, K. Iwasawa, Astronomy & Astrophysics, 455, 1 (2006) 173-185.
[25] A. V. Filippenko, L. C. Ho, The Astrophysical Journal, 588, 1 (2003) L13-L16.
[26] C. A. Onken, B. M. Peterson, M. Dietrich, A. Robinson, I. M. Salamanca, The Astrophysical Journal, 585, 1 (2003) 121-127.